


Defective RNA sensing by RIG-I in severe influenza virus infection

S. E. Jørgensen,* M. Christiansen,[†]
L. B. Ryø,[‡] H. H. Gad,[§] J. Gjedsted,[‡]
P. Staeheli,**¹ J. G. Mikkelsen,[‡]
M. Storgaard,* R. Hartmann[§] and
T. H. Mogensen ^{*,‡2}

*Departments of Infectious Diseases, [†]Clinical Immunology, Aarhus University Hospital,

[‡]Departments of Biomedicine, [§]Molecular Biology and Genetics, Aarhus University,

[‡]Department of Intensive Care, Aarhus University Hospital, Aarhus, Denmark,

**Institute of Virology, Medical Center University of Freiburg, Breisgau, Germany

Present address: ¹Faculty of Medicine, University of Freiburg, Freiburg, Germany
²Department of Clinical Medicine Aarhus University Hospital

Accepted for publication 13 February 2018

Correspondence: T. H. Mogensen, Department of Biomedicine, Aarhus University, Wilhelm Meyers Alle, 8000 Aarhus, Denmark.

E-mail: trinemoge@rm.dk;

Trine.mogensen@biomed.au.dk

Summary

Influenza virus infection causes worldwide seasonal epidemics. Although influenza is usually a mild disease, a minority of patients experience very severe fulminating disease courses. Previous studies have demonstrated a role for type I interferon (IFN) in anti-viral responses during influenza. So far, however, IFN regulatory factor (IRF)7 deficiency is the only genetic cause of severe influenza described in humans. In this study we present a patient with severe influenza A virus (IAV) H1N1 infection during the 2009 swine flu pandemic. By whole exome sequencing we identified two variants, p.R71H and p.P885S, located in the caspase activation and recruitment domain (CARD) and RNA binding domains, respectively, of DExD/H-box helicase 58 (*DDX58*) encoding the RNA sensor retinoic acid inducible gene 1 (RIG-I). These variants significantly impair the signalling activity of RIG-I. Similarly, patient cells demonstrate decreased antiviral responses to RIG-I ligands as well as increased proinflammatory responses to IAV, suggesting dysregulation of the innate immune response with increased immunopathology. We suggest that these RIG-I variants may have contributed to severe influenza in this patient and advocate that RIG-I variants should be sought in future studies of genetic factors influencing single-stranded RNA virus infections.

Keywords: influenza, innate immunity, interferon, RIG-I

Introduction

Influenza virus causes worldwide seasonal epidemics and, occasionally, pandemics. The severity of disease ranges from asymptomatic to very severe fulminating illness with pneumonia and acute respiratory distress syndrome (ARDS), and with an increased risk of bacterial superinfection and pneumonia further complicating the disease course [1,2]. Although most cases of influenza virus infection are self-limiting, an estimated 0.04–0.4% of infected individuals become severely ill during seasonal epidemics, with significant increases during pandemics [2]. Several predisposing factors are known to increase the risk of severe influenza. These include old age, pregnancy, smoking, chronic diseases, such as pulmonary or cardiovascular disease and diabetes, as well as compromised immune responses due to malignancy, therapeutics or HIV infection [1]. Influenza viruses have single-stranded negative-sense

RNA genomes, and most cases of human influenza are caused by influenza A (IAV) and B viruses. The swine flu pandemic in 2009–10 was an IAV H1N1 strain evolved by reassortment in swine [3].

The first line of defence against influenza virus is represented by the innate immune system, in which the induction of interferons (IFN) plays a major role [4,5]. The pattern recognition receptor Toll-like receptor (TLR)7, which recognizes single-stranded RNA (ssRNA), is essential for induction of type I IFN, especially IFN- α , in plasmacytoid dendritic cells (pDCs). This is mediated through activation of the adaptor myeloid differentiation primary response 88 (MyD88) [6,7]. In lung epithelial cells, however, TLR3, which recognizes double-stranded RNA (dsRNA), is involved in sensing of influenza virus and induction of IFN and particularly proinflammatory responses [8,9]. In contrast, the primary inducer of IFN in

non-haematopoietic cells during influenza and other ssRNA virus infections is the cytosolic RNA sensor retinoic acid inducible gene 1 (RIG-I) [10–12].

Following infection with influenza virus, RIG-I recognizes the panhandle structure of the incoming viral ribonucleoproteins (vRNPs) [13]. During subsequent viral transcription and replication further RNA species are produced, which are also detected by RIG-I [14]. Sensing of these RNA species induces RIG-I oligomerization and association with the mitochondrial anti-viral signalling protein (MAVS). This further activates the downstream kinases TANK-binding kinase 1 (TBK1) and I κ B kinase epsilon (IKK ϵ), and subsequently the transcription factors interferon regulatory factor (IRF)3, IRF7 and nuclear factor kappa B (NF- κ B) [15–19], leading ultimately to induction of type I IFN and proinflammatory cytokines. Production of type I IFN results in the induction of numerous IFN-stimulated genes (ISGs), including interferon-inducible Mx protein (MX), ISG56 and IFN-induced transmembrane protein 3 (IFITM3), some of which have been proven to play a major role during influenza infection. For example, transgenic mice expressing the human *MX1* gene exhibit enhanced influenza virus resistance [20].

Several genome-wide association studies (GWAS) have aimed to address the influence of host genetics on the susceptibility and risk of severe disease during influenza virus infection [21–23]. However, overall, most studies have not been sufficiently large and have failed to identify factors of major importance. Finally, and perhaps surprisingly, neither B cell nor T cell deficiencies have been linked directly to an increased susceptibility to influenza. In 2015, a primary immunodeficiency involving the transcription factor IRF7 was found to cause increased susceptibility to severe influenza in a child who developed ARDS due to IAV infection. The IRF7 deficiency was demonstrated to result in decreased production of type I and III IFNs, causing increased viral replication in patient cells [24]. Further evidence of the importance of innate immune responses was provided by a recent publication reporting a role for the RIG-like receptor melanoma differentiation-associated protein 5 (MDA5) in protection against rhinovirus infection in childhood respiratory infections [25].

Here we describe the identification of two heterozygous variants in DExD/H-box helicase 58 (*DDX58*) encoding the cytosolic RNA receptor RIG-I in a 41-year-old Caucasian male patient with severe influenza virus A infection, suggesting that functional defects in RIG-I increase susceptibility to severe influenza infection in humans.

Materials and methods

Patient material and cell lines

The patient described here, a 41-year-old Caucasian male with no previous notable medical history, was one among

12 patients identified based on review of the Extracorporeal Membrane Oxygenation (ECMO) database and medical files, including identification of IAV by polymerase chain reaction (PCR) from throat swabs and a clinical history of severe influenza at the intensive care unit (ICU) at Aarhus University Hospital. The patient provided informed written consent. Patient and volunteer healthy controls were included according to the Helsinki Declaration. All controls, as well as the patient, were non-smokers. Peripheral blood mononuclear cells (PBMCs) were purified by Ficoll density gradient centrifugation from heparinized blood and stored in liquid nitrogen until use. Fibroblasts were isolated from a skin biopsy. PBMCs and fibroblasts were cultured in RPMI-1640 with 10% heat-inactivated fetal bovine serum (HI-FBS) and 1% penicillin–streptomycin. RIG-I knock-out (KO) human embryonic kidney cells 293 (HEK293) cells were grown in Dulbecco's modified Eagle's medium (DMEM) with 10% FBS and 1% penicillin–streptomycin. HEK-blue IFN- α/β cells (Invivogen, Toulouse, France) were cultured in DMEM with 10% FBS, 1% penicillin–streptomycin, 100 μ g/ml Normocin (Invivogen), 30 μ g/ml blasticidin (Invivogen) and 100 μ g/ml zeocin (Invivogen), and for experiments without blasticidin and zeocin. Monocyte-derived macrophages (MDMs) were differentiated from PBMCs in RPMI with 10% HI-FBS, 10% human AB serum, 1% penicillin–streptomycin and 15 ng/ml human macrophage colony stimulating factor (M-CSF) (Peprotech, London, UK). Medium was changed to DMEM with 10% human AB serum, 15 ng/ml M-CSF on days 4 and 7. On day 9 the MDMs were used for experiments.

Whole exome sequencing (WES)

WES was performed using Kapa HTP Library preparation and Nimblegen SeqCap EZ MedExome Plus kit and analysed with Nextseq version 2 chemistry [2 \times 150 base pairs (bp)]. Single nucleotide polymorphisms (SNPs) were called relative to hg19.

Bioinformatics

The variant call files (VCF) were uploaded to Ingenuity variant analysis (IVA; Qiagen, Valencia, VA, USA). Variants were filtered based on rarity (frequency < 0.1%), a gene list based on literature searches on Pubmed, Kyoto Encyclopedia of Genes and Genomes (KEGG) pathways, Online Mendelian Inheritance in Man (OMIM), ClinVar and biological filters in IVA related to influenza infection, immunodeficiency and immune responses. Variants with combined annotation-dependent depletion (CADD) scores < mutation significance cut-off (MSC) scores were excluded [26,27]. After identification of the p.P885S variant in *DDX58*, this gene was searched specifically for the presence of other variants, leading to identification of the more frequent p.R71H variant. Variants identified in IVA

were confirmed by manual inspection of BAM files using the UCSC genome browser. Variants in other genes with possible relevance for influenza infection but judged to be irrelevant in this patient due to low CADD score or high minor allele frequency (MAF) are listed in Supporting information, Table S1 for more information.

Sanger sequencing

gDNA RIG-I was amplified by PCR using the following primers DDX58-R71H forward: 5'-TGTTGGATGTTTCA GGTAGACA-3', DDX58-R71H reverse: 5'-TGGGAA GGTCTGGTGATCCT-3', DDX58-P885S forward: 5'-CACAG GGGGTACAAGCGATCC-3', DDX58-P885S reverse: 5'-A CCCACCTGTTCTTTGCCTC-3' and Phusion Hot Start II DNA polymerase (Thermo Scientific, Waltham, MA, USA). RIG-I variants were confirmed by Sanger sequencing using the following primers R71H-Seq forward: 5'-TCTCA GACTAAGAGGCATG-3', R71H-Seq reverse: 5'-GAGGT GCAGTATATTCAGGC-3' and DDX58-P885S forward, DDX58-P885S reverse.

Ligands and viruses

Human influenza A virus strain A/PR/8/34 (H1N1) (Charles River, Burlington, MA, USA) was used for cell stimulations at multiplicity of infection (MOI) = 0.1, 1 or 2.5 calculated from 50% egg infectious dose (EID₅₀) titre. Human influenza A virus strain A/Hansa/Hamburg/05/09 (H1N1) was used for cell stimulations at MOI = 0.1 calculated from plaque-forming titres on Madin–Darby canine kidney (MDCK) cells. Sendai virus was used at 5 HAU/well. 5'ppp-dsRNA and poly(I:C) (Invivogen) were transfected into cells using lipofectamine 3000 (Invitrogen, Carlsbad, CA, USA) using 1 µg/ml and 2 µg/ml, respectively.

Western blotting

Western blotting was performed as described previously [28]. Primary antibodies were: rabbit anti-RIG-I (AP1900A; Nordic Biosite, Täby, Sweden) 1 : 500; mouse anti-FLAG (F3165-1MG; Sigma Aldrich, St Louis, MO, USA) 1 : 10 000; rabbit anti-glyceraldehyde 3-phosphate dehydrogenase (GAPDH) (FL-335; Santa Cruz Biotechnology, Inc., Dallas, TX, USA) 1 : 10 000; and horseradish peroxidase (HRP)-conjugated anti-beta actin antibody (ab49900; Abcam, Cambridge, UK) 1 : 25.000. Secondary antibodies were: donkey anti-rabbit (711-035-152, lot# 115414; Jackson ImmunoResearch, Newmarket, UK) and donkey anti-mouse (715-036-150, Jackson ImmunoResearch, Newmarket, UK) 1 : 10 000.

DNA isolation

Genomic DNA for WES was isolated from ethylenediamine teraacetic acid (EDTA)-stabilized blood using an EZ1 DNA Blood 350 µl Kit (Qiagen, Hilden, Germany). Genomic

DNA from controls was isolated using the DNeasy Blood and Tissue Kit (Qiagen)

RNA isolation and reverse transcription–quantitative PCR (RT–qPCR)

PBMCs, MDMs and fibroblasts were stimulated or infected with the indicated ligands and viruses for 6 h. Cells were lysed and RNA was purified using the High Pure RNA Isolation Kit (Roche, Basel, Switzerland). cDNA was synthesized using the Quantitect Reverse Transcription Kit (Qiagen) and mRNA expression levels were measured by RT–qPCR using Fastmix II (Quanta Bio, Beverly, MA, USA) and TaqMan primer/probe sets (Life Technologies, Carlsbad, CA, USA), according to the manufacturers' instructions. TaqMan primer/probes were: IFN-β: Hs01077958_s1, C-X-C motif chemokine ligand 10 (CXCL10): Hs01124251_g1, IFN-λ1: Hs00601677_g1, IFN-α2: Hs00265051_s1, interleukin (IL)-6: Hs00985639_m1, tumour necrosis factor (TNF)-α: Hs01113624_g1 DDX58: Hs00204833_m1 TATA binding protein (TBP): Hs00427620_m1, and 18S RNA: Hs03928985_g1.

Type I IFN bioassay

PBMCs were infected with influenza A/PR/8/34 (H1N1) (Charles River) for 24 h and supernatants were collected. HEK blue IFNα/β cells were incubated with PBMC supernatants or IFN-α standards for 24 h. Secreted embryonic alkaline phosphatase (SEAP) protein levels were then measured in HEK blue cell culture supernatants using Quanti-Blue (Invivogen).

Plasmids

R71H and P885S variants were introduced into pEF-BOS/N-FLAG RIG-I WT vector by site-directed mutagenesis using Pfu Ultra II polymerase, with the following primers: R71H-sense: 5'-GGCATCCAAAAAGCCATGGAACCAGCC TTCCTC-3', R71H-anti-sense: 5'-GAGGAAGGCTGGTT CCATGGCTTTTTGGATGCC-3', P885S-sense: 5'-CCACAAAACCTTCAATTTTATAACTGAAATCTCAAATGTCT TGTACTTCACATG-3' and P885S-anti-sense: 5'-CATGTGAAGTACAAGACATTTGAGATTTTCAGTTATAAAAA TTGAAAGTTTTGTGG-3'.

Luciferase reporter assays

RIG-I KO HEK293 T cells were kindly provided by Professor Veit Hornung, Munich [29].

Cells were seeded in 12-well plates and incubated for 24 h. Subsequently, the cells were transfected transiently with IFN-β promoter firefly luciferase reporter plasmid (970 ng/well), β-actin promoter renilla luciferase reporter plasmid (30 ng/well) and either 10 or 1000 ng/well RIG-I WT, R71H, P885S plasmids or plasmids harbouring both of the R71H and P885S variants, as indicated. All transfections were supplemented with pEF-BOS empty plasmid to

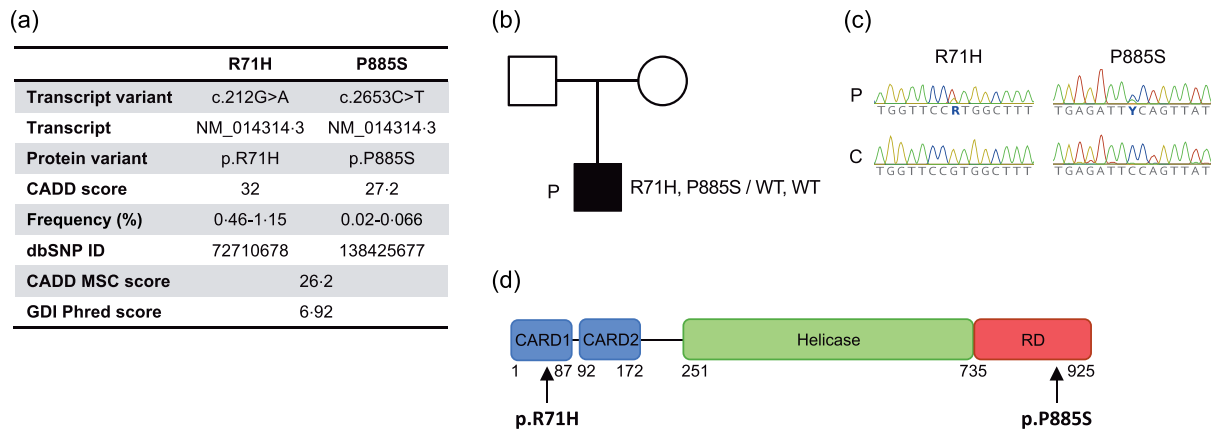


Fig. 1. Identified DEXD/H-box helicase (*DDX58*) variants and domain organization of retinoic acid inducible gene 1 (RIG-I). (a) Table showing characteristics of the *DDX58* variants identified in the patient. The gene damage index (GDI) for *DDX58* is 6.92, which is well below the cut-off of 12.4 proposed for primary immunodeficiencies [30]. The allele frequencies are the European (non-Finnish) frequencies listed in the gnomAD database. (b) Pedigree showing the localization of R71H and P885S variants on the same allele in the patient. (c) Sanger sequencing confirming the R71H and P885S variants in patient (P) versus healthy control (C). (d) RIG-I protein domain structure with R71H and P885S variants indicated. CARD = caspase activation and recruitment domains; RD = regulatory domain. Numbers indicate amino acid residue.

a total of 1000 ng DNA/well. Transfections were performed using polyethylenimine (PEI). After 24 h incubation, cells were infected with 2.5 MOI influenza A/PR/8/34 (H1N1) (Charles River) or 5 HAU SeV. Cells were lysed 18 h post-infection and firefly and renilla luciferase activity measured using Dual Glo (Promega, Madison, WI, USA), according to the manufacturer's instructions.

Statistics

Experiments were performed in experimental duplicates or triplicates, and most experiments were repeated two or three times. The Mann–Whitney rank sum test was used to determine statistical significance: non-significant (n.s.) $P > 0.05$, * $P \leq 0.05$, ** $P \leq 0.01$ and *** $P < 0.001$.

Ethics

The project was approved by the Regional Committee on Health Research Ethics (project no. 1-10-72-251-15) and the Danish Data Protection Agency (project no. 1-16-02-553-15). The patient provided informed written consent.

Results

Identification of two variants in *DDX58* (RIG-I) in a patient with severe influenza

In this study, we enrolled 12 individuals who had been hospitalized previously at the ICU with severe influenza virus infection. WES was performed on all patients, allowing the identification of two variants in *DDX58*, the gene encoding RIG-I in one patient described here (Fig. 1a). For the detailed medical story, see Supplementary information.

The first variant is a SNP (c.212G > A; rs72710678), which causes an amino acid substitution from an arginine to a histidine at position 71 in the RIG-I protein, p.R71H. This variant has a relatively high frequency in the general population of 1.15% (gnomAD database). The other variant (c.2653C > T; rs138425677) causes an amino acid substitution of proline at position 885 to serine, p.P885S. This variant is extremely rare, with a frequency of 0.066% (gnomAD database). The CADD scores of R71H and P885S are 27.2 and 32, respectively, and therefore above the MSC score for *DDX58* of 26.2, indicating that both variants are potentially deleterious for the protein function [26].

Due to the long distance between the two RIG-I variants, it was impossible to determine the specific allelic identity of each variant by WES or conventional Sanger sequencing; moreover, samples from the parents of the patient were not available. Therefore, we cloned RIG-I mRNA from the patient into a vector and performed colony sequencing, revealing that the two variants were located at the same allele, thereby ruling out compound heterozygosity (data not shown). Both variants were confirmed to be heterozygous by Sanger sequencing (Fig. 1c).

RIG-I is a large protein consisting of 925 amino acids. At the N-terminal part of the molecule, two consecutive caspase activation and recruitment domain are located [31]. They are followed by the helicase domain and, finally, the regulatory domain is found at the C-terminal part [31,32]. The R71H variant is located in the first CARD domain, whereas the P885S variant is located in the regulatory domain, the latter of which is involved in 5'ppp-dsRNA binding [33] (Fig. 1d). To examine the impact of the variants on mRNA expression of RIG-I, RT-qPCR was

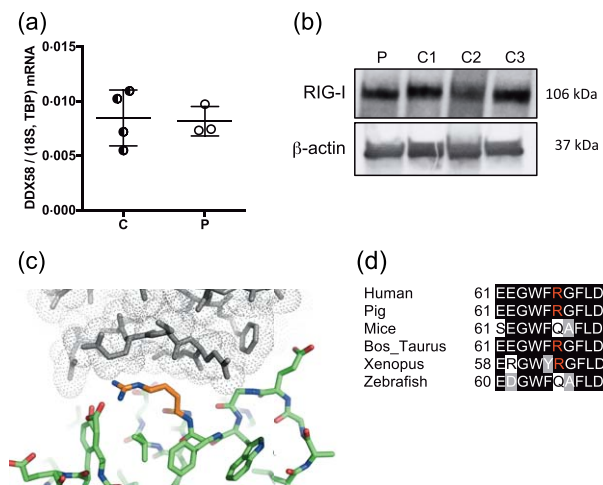


Fig. 2. Expression levels, structure, and evolutionary conservation of retinoic acid inducible gene 1 (RIG-I). (a) RIG-I [DEXD/H-box helicase (DDX58)] mRNA expression measured in patient (P) and control (C) peripheral blood mononuclear cells (PBMCs) by reverse transcription–quantitative polymerase chain reaction (RT–qPCR) and normalized to expression of TATA-binding protein (TBP) and 18S rRNA. (b) RIG-I protein expression measured in patient (P) and control (C1, C2 and C3) PBMCs by Western blotting relative to β-actin. (c) R71 (orange) is localized at the interface between the caspase activation and recruitment domain (CARD) of RIG-I (green) and ubiquitin (grey). R71 is stacked tightly, forming multiple interactions with both other residues in RIG-I and residues in the ubiquitin molecule, which binds to and stabilizes the activated form of the RIG-I CARD domain. Coordinates are from PDB 4NQK. (d) R71 is part of a highly conserved domain. Substitution of R71 with glutamine (Q) is seen in mice and zebrafish; however, due to similar polarity and size, glutamine is assumed to remain compatible with binding of ubiquitin. Results are shown as mean \pm standard deviation (s.d.).

performed and demonstrated similar expression levels in patient cells compared to healthy controls for both PBMCs (Fig. 2a) and fibroblasts (Supporting information, Fig. S1a). Moreover, Western blotting revealed the presence of RIG-I protein in equal amounts in patient PBMCs and controls (Fig. 2b). The crystal structure of RIG-I reveals that R71 makes multiple contacts with both other residues in RIG-I as well as with the ubiquitin chain, and binding of ubiquitin to activated RIG-I stabilizes the activated form of RIG-I and represents a crucial step. The substitution of arginine for histidine in the R71H variant is therefore likely to interfere with this interaction and subsequent signalling from RIG-I (Fig. 2c,d). The P885S variant is located in the C-terminal domain of RIG-I responsible for binding the 5'ppp moiety of unmodified (uncapped) viral RNAs and the change from the sterically restricted proline to the much more flexible serine (Supporting information, Fig. S1b) may potentially affect the stability of the protein structure of this domain.

R71H and P885S variants each decrease RIG-I signalling activity

To investigate the impact of the identified variants on the ability of RIG-I to induce downstream signalling and IFN- β production, we expressed wild-type (WT) RIG-I, either of the two variants or RIG-I harbouring both amino acid substitutions together with two reporter plasmids carrying the IFN- β promoter coupled to firefly luciferase and a β-actin promoter coupled to renilla luciferase in HEK293T cells deficient for endogenous RIG-I expression. Infection with PR8 IAV in cells over-expressing RIG-I showed marked induction of IFN- β promoter activity for WT RIG-I, whereas the activity for the R71H RIG-I mutant was abolished completely and the P885S RIG-I mutant exhibited only minor activity. RIG-I with both variants also showed completely abolished activity (Fig. 3a). In addition, infection with Sendai virus (SeV) induced high IFN- β promoter activity in cells expressing WT RIG-I, whereas significantly less activity was seen in both R71H and P885S RIG-I-expressing cells as well as with RIG-I carrying both variants (Fig. 3b). In line with these findings, over-expression of WT RIG-I (by transfection of 1000 ng plasmid) induced high IFN- β promoter activity on its own, whereas the response for the R71H variant and the combined R71H, P885S RIG-I was abolished almost completely (Fig. 3c). The P885S variant, however, did not alter RIG-I signalling significantly without RNA stimulation (Fig. 3c). Western blotting confirmed the absence of RIG-I in cells transfected with only empty vector. WT, R71H and the R71H, P885S double mutant were all expressed at similar levels, whereas the P885S variant showed slightly decreased expression (Fig. 3d). Taken together, these data demonstrate that the RIG-I variants, particularly the R71H mutation, exert a major impact on the signalling activity causing severely decreased IFN- β inducing ability.

As both variants were heterozygous and located on the same allele, we investigated whether either of the variants might exhibit a dominant negative phenotype. To this end, WT RIG-I was expressed together with increasing amounts of R71H RIG-I (Fig. 3e) or P885S RIG-I (Fig. 3f), together with the two reporter plasmids in HEK293T cells. However, in this cell system, neither of the two variants exerted any dominant negative effect upon the activity of WT RIG-I, thus demonstrating haploinsufficiency of the RIG-I defect in this patient.

Decreased responses to RIG-I ligands in patient cells

To examine further the functional consequences of the variants, we investigated the response to different RIG-I ligands in patient cells. PBMCs from the patient and healthy controls were stimulated with the RIG-I agonist 5'ppp-dsRNA, which has been found to be the optimal RIG-I ligand, and is also found in the panhandle structures of the vRNP of influenza [13,34,35]. Following 5'ppp-

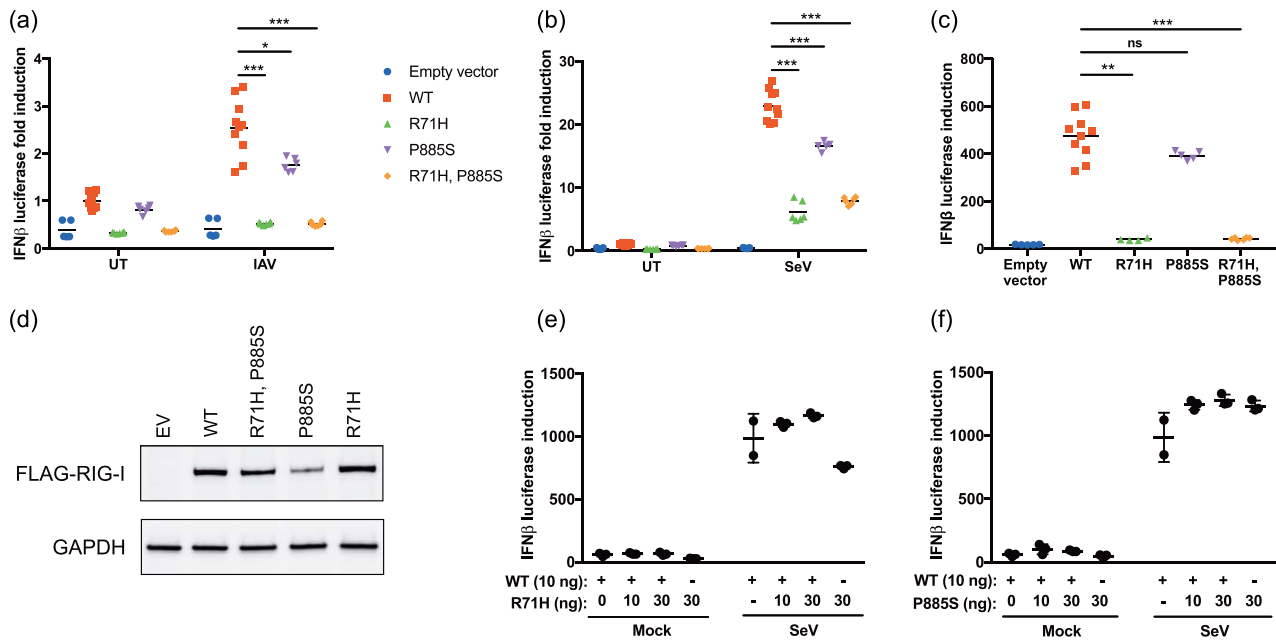


Fig. 3. Expression of mutant and wild-type (WT) retinoic acid inducible gene 1 (RIG-I) in human embryonic kidney cells 293 (HEK293T) cells. RIG-I knock-out (KO) HEK293T cells were transfected transiently with 10 ng of plasmids encoding WT RIG-I, or R71H RIG-I, P885S RIG-I or R71H, P885S RIG-I variants, as indicated; 24 h post-transfection, HEK293T cells were infected with PR8 influenza A virus (IAV) at a multiplicity of infection (MOI) 2.5 (a) or 5 HAU Sendai virus (SeV) (b) for 18 h. Firefly luciferase activity controlled by the interferon (IFN)- β promoter was normalized to renilla luciferase controlled by the β -actin promoter and fold induction was calculated relative to untreated WT. (c) As described in (a) and (b), except that RIG-I KO HEK293T cells were transfected with 1000 ng of RIG-I encoding plasmids without the presence of virus, and data are presented as firefly normalized to renilla. (d) Whole cell lysates from unstimulated HEK293 T cells expressing either empty vector (EV), WT, R71H RIG-I, P885S RIG-I or R71H, P885S RIG-I were immunoblotted to demonstrate levels of RIG-I and GAPDH. (e,f) Similar to (b), except RIG-I KO HEK293T cells were co-transfected with WT and R71H or P885S plasmids as indicated for 24 h and then infected with 5 HAU SeV for 18 h before measurement of luciferase activity. Results are shown as mean \pm standard deviation (s.d.). Statistics were calculated using the Mann-Whitney rank sum test. * $P < 0.05$; ** $P < 0.01$; *** $P < 0.001$; n.s. = not significant.

dsRNA transfection, IFN- β and CXCL10 mRNA responses were measured by RT-qPCR, revealing decreased responses in patient cells (Fig. 4a,b). Next, MDMs were differentiated from patient and control PBMCs and stimulated with another RIG-I agonist poly(I:C). Whereas healthy control MDMs showed very variable responses, patient cells exhibited significantly lower responses than controls as measured by both IFN- β and CXCL10 (Fig. 4c,d). Overall, these data are in line with the previous data, suggesting that the RIG-I variants decrease the ability of RIG-I to induce antiviral and proinflammatory responses to RNA ligands either present in the IAV genome or generated during viral replication in patient cells.

Normal IFN responses in the setting of significantly increased proinflammatory responses to influenza A virus in patients' cells

Patient and control PBMCs were infected with IAV PR8 strain or a clinical isolate from the 2009 pandemic (pdm H1N1), and induction of IFNs and CXCL10 was measured by RT-qPCR. Levels of IFN- β post-infection were similar in patient and control PBMCs (Fig. 5a,d). In contrast, IFN- α 2 and IFN- λ 1 were both expressed at higher

levels in patient PBMCs compared to the two controls when infected with PR8 (Fig. 5b,c), but tended to be largely equal to controls in response to pdm H1N1 (Fig. 5e,f). In addition, production of biologically active type I IFN was examined in supernatants from patient and control PBMCs infected with IAV, revealing a slightly decreased production of active type I IFN, although this did not reach statistical significance (Fig. 5g). For CXCL10, patient PBMCs showed similar levels compared controls when infecting with either PR8 IAV (Fig. 5h) or pdm H1N1 (Fig. 5i). Infection of patient and control MDMs with PR8 IAV confirmed the IFN- β results from the PBMCs, again showing similar expression levels (Fig. 5j).

RIG-I is believed to play a particularly important role in recognition of influenza virus in epithelial cells rather than in haematopoietic cells, and we therefore wanted to investigate the phenotype of cells closer related to the primary site of infection [36]. As we were unable to obtain pulmonary epithelial cells from the patient, instead we isolated patient fibroblasts derived from a skin biopsy. Fibroblasts from the patient and controls were transduced with eGFP-expressing lentivirus and infected subsequently with PR8 IAV at an

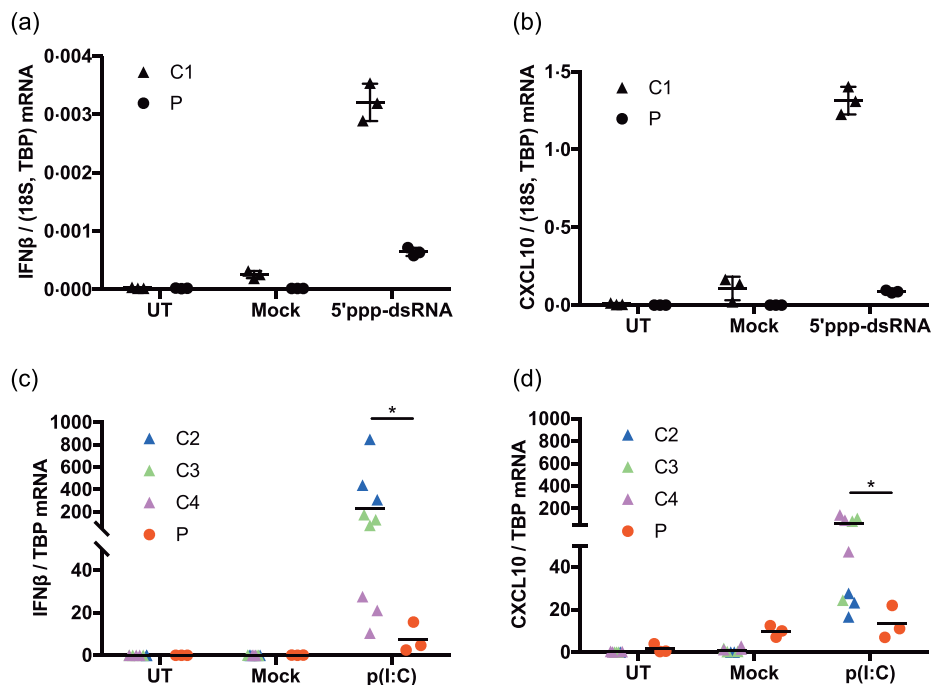


Fig. 4. Anti-viral interferon (IFN) and interferon stimulated gene (ISG) responses to retinoic acid inducible gene 1 (RIG-I) ligands in patient peripheral blood mononuclear cells (PBMCs). Patient (P) and control (C1) PBMCs were transfected with 1 μg/ml 5'ppp-dsRNA for 6 h. IFN-β mRNA (a) and C-X-C motif chemokine 10 (CXCL10) mRNA (b) induction was measured by reverse transcription–quantitative polymerase chain reaction (RT–qPCR) and expression levels were normalized to TATA-binding protein (TBP) and 18S rRNA. Results are experimental triplicates from one experiment, representative of two experiments. Macrophages differentiated from PBMCs from patient (P) and controls (C2, C3, C4) were transfected with 2 μg/ml poly(I:C) for 6 h. IFN-β mRNA (c) and CXCL10 mRNA (d) induction was measured by RT–qPCR and normalized to TBP expression. Results are experimental triplicates of one experiment. Due to limited patient material, the experiment was performed only once. Results are shown as mean ± standard deviation (s.d.). Statistics were calculated using the Mann–Whitney rank sum test. * $P < 0.05$; n.s. = not significant.

MOI of 0.1, as this infectious dose was found to be optimal in fibroblasts. We found that patient PBMCs showed intermediate levels of IFNβ and high levels of IFN-λ1 mRNA, which were not significantly different than those measured in controls (Supporting information, Fig. S2a,b). Of note, the lentiviral transduction did not alter responses to IAV, and in particular did not result in any significant IFN induction by the vector alone (Supporting information, Fig. S2e,f).

As immunopathology constitutes an important aspect of influenza virus pathogenesis, we next examined the expression of two proinflammatory cytokines, TNF-α and IL-6, by RT–qPCR after IAV infection. Importantly, patient PBMCs demonstrated increased baseline levels of both cytokines compared to controls and further increased levels of TNF-α and IL-6 significantly following both PR8 IAV infection (Fig. 6a,b) and pdm H1N1 infection (Fig. 6c,d). Proinflammatory responses were also analysed in patient MDMs which, similarly to patient PBMCs, displayed significantly increased baseline levels of IL-6 and highly increased IL-6 expression compared to controls upon IAV infection (Fig. 6e). When measuring proinflammatory responses in fibroblasts, we found significantly elevated

constitutive and inducible IL-6 levels in patient fibroblasts in response to PR8 IAV, but generally observed low levels of TNF-α and IL-6 in this cell type (Supporting information, Fig. S2c,d).

In summary, these data demonstrate that patient PBMCs, MDMs and fibroblasts mount essentially normal interferon responses, but significantly increased proinflammatory responses upon IAV infection compared to controls *in vitro*.

Discussion

Here we present a study identifying two variants in the *DDX58*-encoded cytosolic RNA sensor RIG-I in an adult Caucasian male patient who developed severe influenza infection during the H1N1 swine flu pandemic in 2009–10.

The RIG-I R71H variant is located in the first CARD domain of RIG-I which, together with the second CARD domain, is responsible for oligomerization of RIG-I and interaction with the downstream adaptor MAVS [15]. Our results agree with a model according to which the R71H variant prevents a stable interaction with ubiquitin and thus destabilizes RIG-I oligomers. The other variant identified at

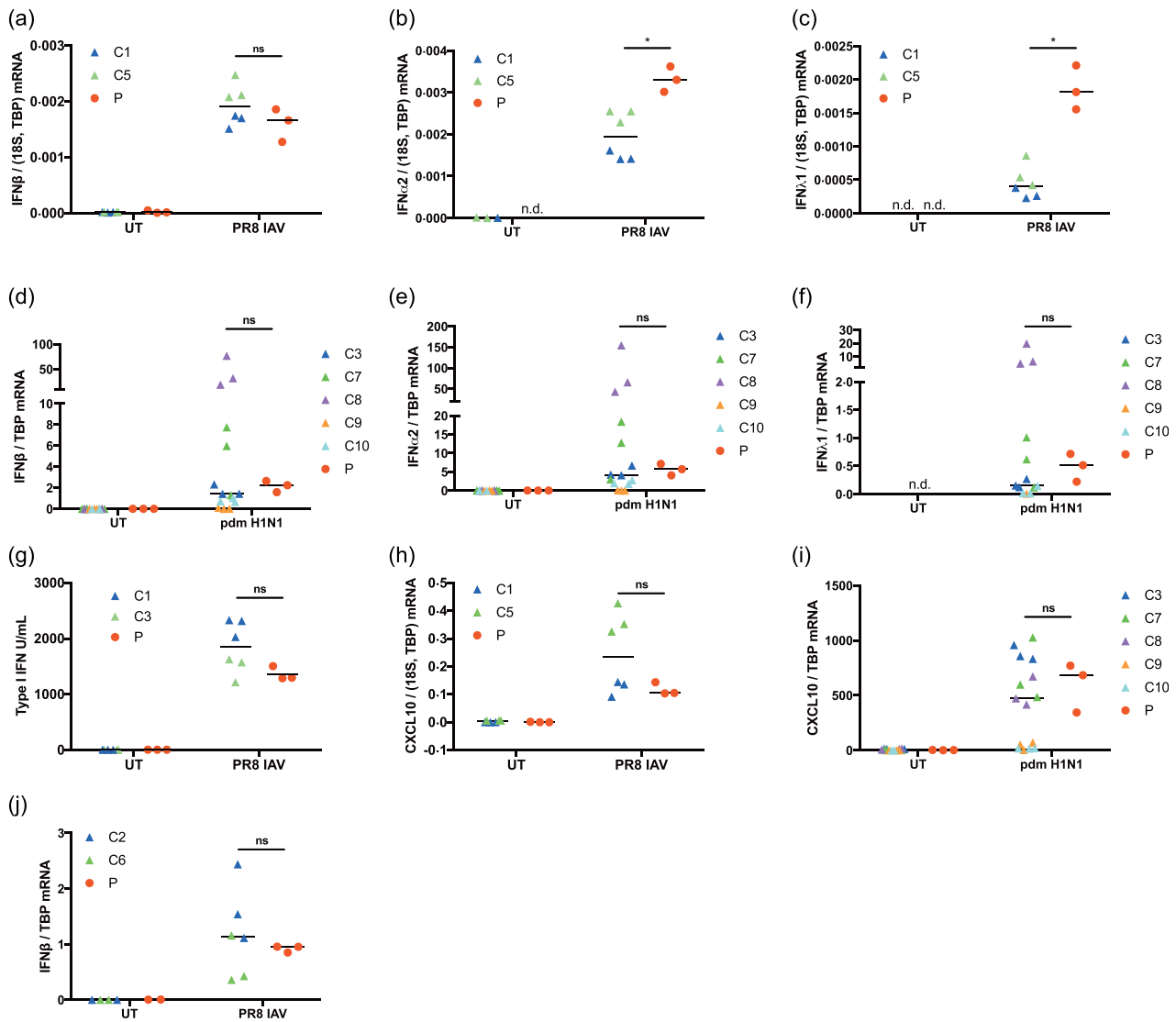


Fig. 5. Anti-viral interferon (IFN) responses to influenza A virus (IAV) in patient peripheral blood mononuclear cells (PBMCs) and macrophages. PBMCs from patient (P) and healthy controls (C1, C3, C5, C7–C10) were infected with PR8 influenza A virus (PR8 IAV) at a multiplicity of infection (MOI) 1 or a clinical isolate from the 2009 pandemic (pdm H1N1) at MOI 0.1 for 6 h. IFN- β (a,d), IFN- α 2 (b,e), IFN- λ 1 (c,f) and C-X-C motif chemokine 10 (CXCL10) (h,i) responses were measured by reverse transcription–quantitative polymerase chain reaction (RT–qPCR) and normalized to expression of 18S rRNA and/or TATA-binding protein (TBP). Results are experimental triplicates from one experiment, representative of two independent experiments (a–c,h) or experimental triplicates from one experiment (d–f,i). (g) PBMCs from patient and healthy controls (C1, C3) were infected with PR8 IAV at MOI 0.1 for 24 h. Supernatants were harvested and levels of active type I IFN were measured by an IFN bioassay. Results are experimental triplicates from one experiment, representative of two independent experiments. Monocyte-derived macrophages from patient and healthy controls (C2, C6) were infected with PR8 IAV at MOI 1 for 14 h. IFN- β (j) responses were measured by RT–PCR and normalized to expression of TBP. Results are experimental triplicates from one experiment, representative of two individual experiments. Overall median (controls) and median (patient) is indicated by the black line in panel (a–i). Overall mean and mean are indicated by the black lines in panel (j). Statistics were calculated using Mann–Whitney rank sum test. * $P < 0.05$; n.s. = not significant.

the P885 residue is located within the 5'ppp-RNA binding domain, and the rigidity of this domain is lost when proline is substituted with serine, possibly affecting the stability of the 5'ppp-RNA binding domain and hence lowering the affinity for 5'ppp-RNAs. This scenario would be predicted to cause impaired recognition of 5'ppp-RNAs and decreased signalling activity, as observed in the luciferase

reporter assays. As the R71H variant was demonstrated to exert severely decreased signalling activity, both in the presence of dsRNA and independently of dsRNA, the mechanism by which this occurs may be through impaired RIG-I oligomerization and interaction with MAVS. Given that we did not observe any dominant negative effect of neither of the RIG-I variants upon WT RIG-

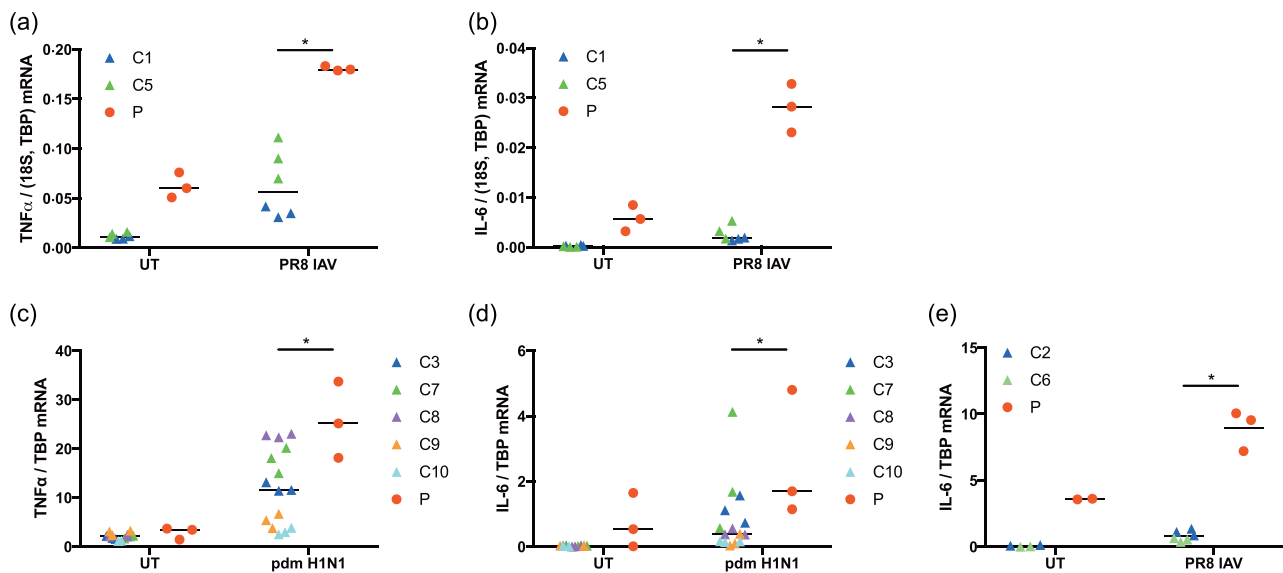


Fig. 6. Inflammatory responses to influenza A virus (IAV) in patient peripheral blood mononuclear cells (PBMCs) and macrophages. PBMCs from patient (P) and healthy controls (C1, C3, C5, C7–C10) were infected with PR8 influenza A virus (PR8 IAV) at a multiplicity of infection (MOI) 1 or a clinical isolate from the 2009 pandemic (pdm H1N1) at MOI 0.1 for 6 h. TNF- α (a,c), and interleukin (IL)-6 (b,d) responses were measured by reverse transcription–quantitative polymerase chain reaction (RT–qPCR) and normalized to expression of 18S rRNA and/or TATA-binding protein (TBP). Results are experimental triplicates from one experiment (a,b), representative of two independent experiments or experimental triplicates from one experiment (c,d). Monocyte-derived macrophages from P and C2, C6 were infected with PR8 IAV at MOI 1 for 14 h. IL-6 (e) responses were measured by RT–PCR and normalized to expression of TBP. Results are experimental triplicates from one experiment. Overall median (controls) and median (patient) are indicated by black lines. Statistics were calculated using the Mann–Whitney rank sum test. * $P < 0.05$; n.s. = not significant.

I, we propose that the underlying mechanism involves haploinsufficiency in the patient.

Transfection of patient PBMCs and MDMs with the RIG-I ligands 5'ppp-dsRNA and poly(I:C), respectively, demonstrated decreased responses compared to healthy controls, indicating that the impaired signalling ability of RIG-I observed in the experimental HEK293T cell-based luciferase reporter assay also manifests in patient cells. Infection of patient PBMCs with IAV, however, did not demonstrate decreased IFN and CXCL10 responses. As haematopoietic cells mainly utilize other pattern recognition receptors (PRRs) than RIG-I during influenza infection [6,7,12], the normal production of IFN- β and CXCL10 in patient PBMCs might reflect the existence of redundancy, i.e. the scenario that receptors such as TLR7 serve instead as the primary inducer of IFN responses to IAV in haematopoietic cells. In contrast, RIG-I is believed to play a central role in induction of IFN responses to IAV in fibroblasts and epithelial cells [10,11]. However, fibroblasts isolated from patient skin showed intermediate expression levels of types I and III IFN after IAV infection. Although fibroblasts are probably more similar to lung epithelial cells than PBMCs with regard to expression and utilization of different PRRs, these cell types are not identical. A distinctive cellular phenotype might therefore be revealed by examination of patient lung epithelial cells, which unfortunately were not available to us in the present study.

A major finding of the present study was data showing that patient PBMCs exhibited significantly increased expression of the proinflammatory cytokines TNF- α and IL-6 upon infection with either of the two different IAV strains compared to controls, and with a similar pattern observed for patient fibroblasts and MDMs. Indeed, previous studies in mice have suggested a dysregulation of inflammatory pathways during influenza infection in RIG-I-deficient cells, as genes involved in apoptosis, TLR and IL-1 signalling and induction of proinflammatory responses were found to be up-regulated during influenza infection [11]. Additionally, a recent study provided evidence of up-regulated expression of the proinflammatory cytokines IL-6, IL-8 and TNF- α by IAV infection in RIG-I-deficient lung epithelial cells [25]. Based on these data, we speculate that RIG-I deficiency may result in elevated proinflammatory responses causing exaggerated immunopathology in the lungs, possibly secondary to increased IAV replication. This scenario would be predicted to translate into a more severe course of disease consistent with the well-recognized role of immunopathology in severe influenza [37]. In line with this idea, TLR3 induces mainly proinflammatory responses during influenza infection of lung epithelial cells [9], and indeed TLR3-deficient mice have decreased inflammation and mortality compared to WT mice [38]. Therefore, impaired RIG-I responses might lead to increased proinflammatory responses, mediated

possibly through TLR3 and TLR7 recognition of viral dsRNA or ssRNA, respectively, leading to enhanced immunopathology and lung injury during influenza infection.

As we did not observe a significant phenotype in patient cells with respect to decreased anti-viral IFN responses to IAV, it is not possible to conclude with certainty that the identified RIG-I variants are direct causes of the severe disease course experienced by the patient. However, based on the finding of considerable signaling deficiency exhibited by the RIG-I variants with regard to induction of IFN- β , combined with the findings of consistently significantly increased proinflammatory cytokine responses in patient PBMCs, macrophages and fibroblasts compared to controls, we suggest that the discovered variants exert an important role upon viral recognition and generation of appropriate anti-viral and proinflammatory responses. Moreover, these data underscore the importance of studying further the essential role of inflammatory responses causing pathology during influenza.

Our finding that IFN production from PBMCs and MDMs in response to IAV from patients was largely similar to that from control PBMCs, despite data demonstrating impaired IFN induction in HEK293 cells expressing these RIG-I mutants, may seem surprising. One explanation for this apparent paradox may be the existence of redundancy in pathogen recognition of IAV as a major determinant for whether the RIG-I defect translates into a cellular phenotype with respect to IFN production in a given cell type. In epithelial cells, in which RIG-I plays an essential and dominant role in IAV recognition, a mutation in the RIG-I encoding gene *DDX58* impairing the signalling capacity of RIG-I is more likely to result in reduced IFN responses *in vitro*. Indeed, epithelial cells are the prime targets for infection by IAV in the respiratory tract, and if these cell types do not mount sufficient anti-viral IFN responses early during infection, this may result in subsequent increased viral load, exaggerated inflammatory responses, immunopathology and a severe disease course.

In conclusion, we therefore advocate that the presence of the R71H and P885S variants should be investigated in future studies on genetic susceptibility to severe disseminated infection with IAV and other ssRNA viruses, to which RIG-I signalling is believed to play a major role. This approach will contribute to clarifying further the role of defects in RIG-I and other RNA-recognizing PRRs in increased susceptibility to severe viral infection in humans.

Author contributions

S. E. J., M. S. and T. H. M. conceived the idea and designed the project. S. E. J., J. G. and M. S. identified and included patients. P. S. isolated and contributed with the clinical isolate of IAV. S. E. J., M. C., H. H. G., L. B. R., J. G. M., R. H. and T. H. M. designed and analysed experiments. S. E. J., M. M., H. H. G. and K. A. S. performed experiments.

M. C. was involved in analysis of the WES data. S. E. J. and T. H. M. drafted the first version of the manuscript (with input from M. C. and R. H.). All authors read and approved the final version of the manuscript.

Acknowledgements

This work was supported by the Lundbeck Foundation (R151-2013-14668); the Kong Christian den Tiendes Fond; and Christian Larsen og Dommer Ellen Larsens Legat to S. E. J., the Danish Council for Independent Research (4004-00047B); Aarhus University Research Fund (AUFF-E-2015-FLS-66); and the Simon Fougner Hartmanns Fond to T. H. M. We thank the patient and healthy controls for participating in the study and laboratory technician Bente Ladegaard and Christian Knudsen for technical assistance.

Disclosure

The authors have no conflicts of interest to declare

References

- 1 Paules C, Subbarao K. Influenza. *Lancet* 2017; **390**:697–708.
- 2 Ciancanelli MJ, Abel L, Zhang SY, Casanova JL. Host genetics of severe influenza: from mouse Mx1 to human IRF7. *Curr Opin Immunol* 2016; **38**:109–20.
- 3 Taubenberger JK, Kash JC. Influenza virus evolution, host adaptation, and pandemic formation. *Cell Host Microbe* 2010; **7**:440–51.
- 4 Garcia-Sastre A. Induction and evasion of type I interferon responses by influenza viruses. *Virus Res* 2011; **162**:12–8.
- 5 Galani IE, Triantafyllia V, Eleminiadou EE *et al*. Interferon-lambda mediates non-redundant front-line antiviral protection against influenza virus infection without compromising host fitness. *Immunity* 2017; **46**:875–90.e6.
- 6 Lund JM, Alexopoulou L, Sato A *et al*. Recognition of single-stranded RNA viruses by Toll-like receptor 7. *Proc Natl Acad Sci USA* 2004; **101**:5598–603.
- 7 Diebold SS, Kaisho T, Hemmi H, Akira S, Reis e Sousa C. Innate antiviral responses by means of TLR7-mediated recognition of single-stranded RNA. *Science* 2004; **303**:1529–31.
- 8 Wu W, Zhang W, Duggan ES, Booth JL, Zou MH, Metcalf JP. RIG-I and TLR3 are both required for maximum interferon induction by influenza virus in human lung alveolar epithelial cells. *Virology* 2015; **482**:181–8.
- 9 Le Goffic R, Pothlichet J, Vitour D *et al*. Cutting edge: influenza A virus activates TLR3-dependent inflammatory and RIG-I-dependent antiviral responses in human lung epithelial cells. *J Immunol* 2007; **178**:3368–72.
- 10 Kato H, Takeuchi O, Sato S *et al*. Differential roles of MDA5 and RIG-I helicases in the recognition of RNA viruses. *Nature* 2006; **441**:101–5.
- 11 Loo YM, Fornek J, Crochet N *et al*. Distinct RIG-I and MDA5 signaling by RNA viruses in innate immunity. *J Virol* 2008; **82**:335–45.
- 12 Kato H, Sato S, Yoneyama M *et al*. Cell type-specific involvement of RIG-I in antiviral response. *Immunity* 2005; **23**:19–28.
- 13 Liu G, Park HS, Pyo HM, Liu Q, Zhou Y. Influenza A virus panhandle structure is directly involved in RIG-I activation and interferon induction. *J Virol* 2015; **89**:6067–79.

- 14 Baum A, Garcia-Sastre A. Differential recognition of viral RNA by RIG-I. *Virulence* 2011; **2**:166–9.
- 15 Wu B, Peisley A, Tetrault D *et al.* Molecular imprinting as a signal-activation mechanism of the viral RNA sensor RIG-I. *Mol Cell* 2014; **55**:511–23.
- 16 Kawai T, Takahashi K, Sato S *et al.* IPS-1, an adaptor triggering RIG-I- and Mda5-mediated type I interferon induction. *Nat Immunol* 2005; **6**:981–8.
- 17 Seth RB, Sun L, Ea CK, Chen ZJ. Identification and characterization of MAVS, a mitochondrial antiviral signaling protein that activates NF- κ B and IRF 3. *Cell* 2005; **122**:669–82.
- 18 Meylan E, Curran J, Hofmann K *et al.* Cardif is an adaptor protein in the RIG-I antiviral pathway and is targeted by hepatitis C virus. *Nature* 2005; **437**:1167–72.
- 19 Xu LG, Wang YY, Han KJ, Li LY, Zhai Z, Shu HB. VISA is an adapter protein required for virus-triggered IFN- β signaling. *Mol Cell* 2005; **19**:727–40.
- 20 Deeg CM, Hassan E, Mutz P *et al.* *In vivo* evasion of MxA by avian influenza viruses requires human signature in the viral nucleoprotein. *J Exp Med* 2017; **214**:1239–48.
- 21 Cheng Z, Zhou J, To KK *et al.* Identification of TMPRSS2 as a susceptibility gene for severe 2009 pandemic A(H1N1) influenza and A(H7N9) influenza. *J Infect Dis* 2015; **212**:1214–21.
- 22 Chen Y, Zhou J, Cheng Z *et al.* Functional variants regulating LGALS1 (Galectin 1) expression affect human susceptibility to influenza A(H7N9). *Sci Rep* 2015; **5**:8517.
- 23 Allen EK, Randolph AG, Bhangale T *et al.* SNP-mediated disruption of CTCF binding at the IFITM3 promoter is associated with risk of severe influenza in humans. *Nat Med* 2017; **23**:975–83.
- 24 Ciancanelli MJ, Huang SX, Luthra P *et al.* Infectious disease. Life-threatening influenza and impaired interferon amplification in human IRF7 deficiency. *Science* 2015; **348**:448–53.
- 25 Lamborn IT, Jing H, Zhang Y *et al.* Recurrent rhinovirus infections in a child with inherited MDA5 deficiency. *J Exp Med* 2017; **214**:1949–72.
- 26 Itan Y, Shang L, Boisson B *et al.* The mutation significance cut-off: gene-level thresholds for variant predictions. *Nat Methods* 2016; **13**:109–10.
- 27 Kircher M, Witten DM, Jain P, O’Roak BJ, Cooper GM, Shendure J. A general framework for estimating the relative pathogenicity of human genetic variants. *Nat Genet* 2014; **46**:310–5.
- 28 Andersen LL, Mork N, Reinert LS *et al.* Functional IRF3 deficiency in a patient with herpes simplex encephalitis. *J Exp Med* 2015; **212**:1371–9.
- 29 Zhu J, Zhang Y, Ghosh A *et al.* Antiviral activity of human OASL protein is mediated by enhancing signaling of the RIG-I RNA sensor. *Immunity* 2014; **40**:936–48.
- 30 Itan Y, Shang L, Boisson B *et al.* The human gene damage index as a gene-level approach to prioritizing exome variants. *Proc Natl Acad Sci USA* 2015; **112**:13615–20.
- 31 Yoneyama M, Kikuchi M, Natsukawa T *et al.* The RNA helicase RIG-I has an essential function in double-stranded RNA-induced innate antiviral responses. *Nat Immunol* 2004; **5**:730.
- 32 Saito T, Hirai R, Loo YM *et al.* Regulation of innate antiviral defenses through a shared repressor domain in RIG-I and LGP2. *Proc Natl Acad Sci USA* 2007; **104**:582–7.
- 33 Cui S, Eisenacher K, Kirchhofer A *et al.* The C-terminal regulatory domain is the RNA 5'-triphosphate sensor of RIG-I. *Mol Cell* 2008; **29**:169–79.
- 34 Hornung V, Ellegast J, Kim S *et al.* 5'-Triphosphate RNA is the ligand for RIG-I. *Science* 2006; **314**:994–7.
- 35 Pichlmair A, Schulz O, Tan CP *et al.* RIG-I-mediated antiviral responses to single-stranded RNA bearing 5'-phosphates. *Science* 2006; **314**:997–1001.
- 36 Iwasaki A, Pillai PS. Innate immunity to influenza virus infection. *Nat Rev Immunol* 2014; **14**:315–28.
- 37 Damjanovic D, Small C-L, Jeyanathan M, Jeyanathan M, McCormick S, Xing Z. Immunopathology in influenza virus infection: uncoupling the friend from foe. *Clin Immunol* 2012; **144**:57–69.
- 38 Le Goffic R, Balloy V, Lagranderie M *et al.* Detrimental contribution of the Toll-like receptor (TLR)3 to influenza A virus-induced acute pneumonia. *PLoS Pathog* 2006; **2**:e53.

Supporting information

Additional Supporting information may be found in the online version of this article at the publisher’s web-site:

Table S1. List of gene variants, allele frequency and combined annotation dependent depletion (CADD) score from whole exome sequencing (WES) analysis of the patient (0.1% frequency cut-off, CADD > 15).

Fig. S1. (a) Retinoic acid inducible gene 1 (RIG-I) [DEXD/H-box helicase 58 (DDX58)] mRNA expression measured in patient (P) and control (C) fibroblasts by reverse transcription–quantitative polymerase chain reaction (RT–qPCR) and normalized to expression of TATA-binding protein (TBP). (b) P885 (orange) is situated in the central beta-strand in the C-terminal domain of RIG-I (PDB code 2YKG). The strand is curved and this curvature is expected to be influenced by a substitution of P to S.

Fig. S2. Primary dermal fibroblasts isolated from patient (P) and controls (F1, F2, F3, F4) skin biopsies were transduced with enhanced green fluorescent protein (eGFP)-expressing lentiviral vectors for 24 h and subsequently infected with 0.1 multiplicity of infection (MOI) PR8 influenza A virus (IAV) for 6 h. mRNA levels of interferon (IFN)- β (a), IFN- λ 1 (b), tumour necrosis factor (TNF)- α (c) and interleukin (IL)-6 (d) were measured by reverse transcription–quantitative polymerase chain reaction (RT–qPCR) and normalized to expression of TATA-binding protein (TBP). Results are experimental triplicates (controls) and duplicates (patient) from one experiment. Due to limited patient material the experiment was only performed once. Black line indicates grand mean (controls) and mean (patient). (e,f) Control fibroblasts were left untreated or transduced with eGFP expressing lentivector; 48 h upon transduction the fibroblasts were infected with 0.1 MOI PR8 IAV for 6 h. RT–qPCR was used to measure expression levels of IFN and C-X-C motif chemokine 10 (CXCL10). Statistics were calculated using the Mann–Whitney rank sum test. * P < 0.05; n.s. = not significant.